PHILOSOPHICAL TRANSACTIONS OF THE ROYAL SOCIETY B BIOLOGICAL SCIENCES

Electron Microscopic Studies of Macromolecules Without Appositional Contrast

A. K. Kleinschmidt

Phil. Trans. R. Soc. Lond. B 1971 **261**, 143-149
doi: 10.1098/rstb.1971.0045

Phil. Trans. Roy. Soc. Lond. B. **261**, 143–149 (1971) [143]
Printed in Great Britain

Electron microscopic studies of macromolecules without appositional contrast

By A. K. Kleinschmidt
Department of Biochemistry, New York University School of Medicine, New York, U.S.A.

[Plates 27 to 29]

Dedicated to the memory of Nicole Granboulan

In pursuing electron microscopic studies of individual biomacromolecules without contrast-enhancing stains, conventional transmission electron microscopy was improved by the use of thin, large area carbon support films. Contrast of the bright-field appearance of the unstained macromolecules and complexes was strongly enhanced in a dark field obtained by insertion of a dark-field objective aperture or by tilting the condenser system. The results are exemplified by various biological macromolecules such as DNA–protein monolayers or ferritin molecules.

Bright- and dark-field microscopy

A biological macromolecule composed of many covalently bound atoms is organized to a tertiary structure by weak bonds. In order to observe the structure in conventional high-resolution electron microscopy, the hydrated small object is converted to a dehydrated particle supported by a thin carbon film. Additional contrast is usually obtained by deposition of a metal shadow and/or by using electron-dense stains. In such electron micrographs, the resolution of detailed structure usually does not extend below 2 nm (20 Å). In this study, attempts have been made to observe biomacromolecules without the use of appositional contrast. The instrumental approach is bright- and dark-field electron microscopy of unstained biomacromolecules.

There are two major ways in which electrons contribute to the image formation of macromolecules:

First, the illuminating electron beam, at accelerating voltages between 50 and 100 kV, interacts with the molecular object to produce a *bright-field image*. A small fraction of electrons is scattered 'amorphously' (Hall 1966) and part of it excluded from the in-focus image by the objective aperture (figure 1*a*) and lens design. Undeflected electrons and those scattered electrons that pass through the objective aperture generate an image at the photographic plate. The contrast in this image is due to the amplitude contrast *and* phase contrast (see Heidenreich 1964*a*).

Secondly, a dark-field image is produced predominantly by electrons elastically scattered from within the range of the object, while the undeflected electron beam is eliminated (Heidenreich 1964*b*). Since most of the inelastically scattered electrons travel with the centre beam of unscattered electrons (zero-order electron beam), inelastically scattered electrons contribute to a much less extent to the image. This is as if a second distorted low contrast image were overlaid, like a haze on to the primary dark-field image produced by elastically scattered electrons.

At present, various types of dark field can be used. A dark field is formed either by a *dark-field condenser system* (figure 1*b*), by a *tilt* (figure 1*c*) of the electron gun condenser system, or by

a *dark-field objective aperture* (figure 1*d*) positioned in or close to the back-focal plane of the objective lens.

The image contrast obtained differs profoundly in bright field and dark field as shown in a simple qualitative way in figure 2. The electron density distribution (ΔE) in the image of a small amorphous object produces a small decremental contrast in bright field, and a hole is

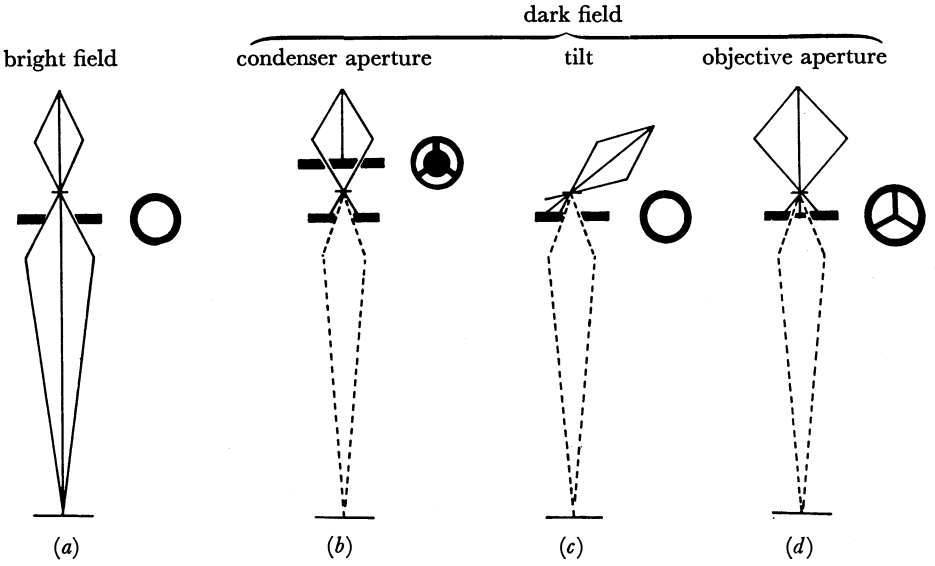

FIGURE 1. Schematic instrumental lay-out for bright- and dark-field electron microscopy. (*a*) *Conventional bright field.* The objective aperture (30, 40, or 50 μm ϕ) is assumed to be in or close to the back-focal plane of the objective lens. The final image is formed by a two-stage (objective-projector) or a three-stage (objective-intermediate lens-projector) lens system. (*b*) *Dark-field condenser aperture* can be set at various positions of the condenser system (Dupouy, Perrier & Verdier 1966). The ring-shaped illumination favours minimum damage to the object (Stoeckenius 1970). (*c*) The *tilt* in the gun-condenser system is produced mechanically (Ottensmeyer 1969) or by using an electromagnetic beam deviation system. The objective aperture is of regular size (50 or 30 μm diameter). (*d*) *Dark-field objective apertures* (beam stop) of various forms are positioned at the back-focal plane (Thon 1968) or adjustable in the objective lens system (Dupouy *et al.* 1969).

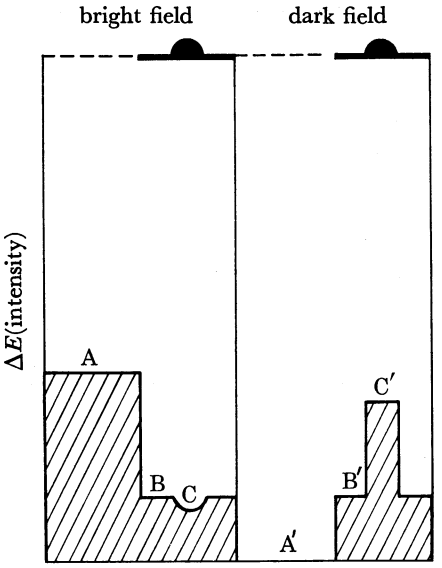

FIGURE 2. Bright- and dark-field contrast. A qualitative sketch of electron intensity in the conventional bright-field and ideal dark-field. A and A′ image of a hole; B and B′ image of the carbon support film; C and C′ image of a small object cross-sectioned in the upper graph. The contrast differences are explained in the text.

PHILOSOPHICAL TRANSACTIONS OF THE ROYAL SOCIETY B BIOLOGICAL SCIENCES

imaged with maximum electron density. In dark field, however, a small object shows high incremental contrast due solely to the scattering of electrons. In perfect dark field, the image of a hole is completely free of electrons and appears 'black'. From these findings, it is immediately obvious that in dark field the carbon film thickness and structure are important factors in image formation of a carbon-supported object of limited size.

The electron microscope should be alined properly and the astigmatism corrected. This correction can be conveniently performed by means of the stigmator control while small holes in a thick carbon film are observed in bright field. In bright field, a hole in a 'holey' carbon film appears with fringes in defocused position (figure 3, plate 27, upper row, left and right, $\Delta f = 20$ nm; middle position = focus). When converted to a dark-field by mechanical tilt of the condenser system (Ottensmeyer 1969), a focus series (figure 3, middle and lower row, each step $\Delta f = 20$ nm) of these holes shows that an in-focus image of such a holey, thick support film is difficult to visualize in dark field. Thus, dark-field imaging of thick films is not the proper way to aline the astigmatism. Extremely thin holey systems, however, allow the edges in dark field to be focussed with high accuracy due to a scattering of electrons at the border.

Carbon support films

Thin support films are mandatory for bright- and dark-field observations of unstained macromolecules. To produce films covering a large area, electron specimen mounts (platinum grids of Siemens type with 70 μm round holes) were used exclusively (figure 4). On these Pt grids is mounted a heavy collodion layer coated on top with the carbon support film of appropriate thickness (< 7 nm) (Reimer 1967). After the specimen preparation is completed, the collodion layer is removed ('puffed-off') in a clean oven at 180 °C or at a higher temperature.

This heating process, which causes a retraction of the collodion layer toward the edges of the 70 μm hole of the Pt grids, does not harm the thin carbon film as judged by microscopy. By observation with an episcopic light microscope (Zeiss Photomicroscope, $\times 25$ episcopic objective Epiplan (HD)), the quality of such carbon support films can easily be controlled. The carbon support film should be almost invisible, but minute particulate matter which often accidentally contaminates the support film produce hazy contrast showing minute spots in reflected light. The thick carbon–collodion layers appear more diffuse in the light microscope. Under normal circumstances, however, the deposited macromolecules are not detectable.

The thickness of the evaporated carbon film is judged by the contrast produced on lens paper after the carbon is evaporated in the high vacuum of a metal evaporator (Balzers BA 350S). The accuracy of the deposition process can be profoundly improved by using a quartz crystal thin film monitor (Balzers QSG 101) which allows slow evaporation and estimation of minimum amounts of carbon deposited.

Thin carbon films of smaller areas are prepared on holes in a perforated collodion film which usually is carbon reinforced and mounted on copper grids. As with the case of Pt grids, a thin collodion layer is mounted on the holey system and coated with an extremely thin carbon film (often less than 3 nm thick). By heating these preparations up to about 220 °C, the second collodion layer is puffed off before depositing the preparation. The support film is then ready to transfer macromolecules from solution. The stability of these small range films depends very much on the size and concentration of holes in the initial perforated film. Various methods for preparing of perforated films have been described (see Bradley 1965; Ottensmeyer 1969).

PHILOSOPHICAL TRANSACTIONS OF THE ROYAL SOCIETY B BIOLOGICAL SCIENCES

Mounting the preparations

The preparative steps in mounting unstained macromolecules for bright- and dark-field microscopy are important when detailed structure ranging from 10 to 0.5 nm is to be studied. Since appropriate carbon thickness and sufficient stability are the most critical conditions for high-resolution electron microscopy of mounted molecules, a series of support films varying in the carbon support thickness are prepared, from which one is selected for stability and minimum thickness.

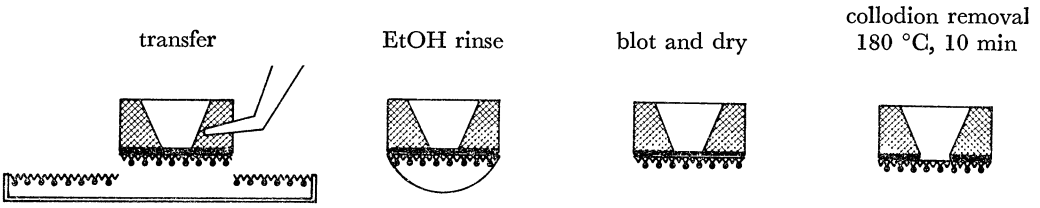

FIGURE 4. Preparation scheme of transfer and drying. The DNA-protein monolayer is transferred to the carbon–collodion support mounted on a Pt-grid and then the adherent droplet of the aqueous hypophase replaced by touching the surface of ethanol (10 ml). This dehydrates the monolayer adsorbed to the carbon top film. After blotting with filter-paper, the carbon surface dries rapidly. Collodion is removed in a clean oven at 180 °C for 10 min. The remaining carbon support film can be prepared as a freely supported carbon layer of a few nanometres in thickness.

(i) The nucleic acid–protein monolayer techniques (Kleinschmidt 1968) require large areas of support film to observe sizeable nucleic acid filaments. They are studied under various conditions of native or partly denatured molecules (see Lang, this volume, p. 151). The sequence of preparative steps in mounting the preparation is illustrated in figure 4. When touching the surface of the nucleic acid–protein film with a horizontally held grid, film aliquots are transferred to the carbon–collodion support. The adherent droplet of the hypophase is replaced by ethanol, blotted and dried.

For comparison, stained preparations are prepared as follows: after film transfer, the adherent droplet of the hypophase is replaced by water followed by a staining process with 0.1 mmol l^{-1} uranyl acetate in acetone + 2 % methanol (1 min) (Gordon & Kleinschmidt 1968) which has been shown to yield high-contrast staining of nucleic acids. The final preparation step for stained and unstained preparations is always the removal of the collodion in a hot clean oven at 180 °C.

(ii) Protein complexes are usually prepared in a minimum salt concentration necessary to maintain the physical structure. Adequate dilution immediately before mounting yields protein concentrations in the range below 10 μg/ml. In many instances, structural details can be maintained by means of a 'prefixation' *in vitro* by formaldehyde or glutaraldehyde. To reduce excess salt and aldehyde, it is preferable to rinse the adsorbed preparation briefly with water. We usually avoid ethanol treatment which may have denaturing effects on the quarternary structure of adsorbed proteins.

(iii) In the preparation of ribosomes and complex particles or ribosomal subunits, we also use droplets deposited on extremely thin carbon support films. Prefixation is often mandatory (Shelton & Kuff 1966); high sucrose concentration should be avoided by dialysis of the preparation against the proper Mg^{2+} concentration. The adherent water is removed by blotting; minimal damage apparently occurs when the rinse with water or with ethanol is omitted.

PHILOSOPHICAL TRANSACTIONS OF THE ROYAL SOCIETY B BIOLOGICAL SCIENCES

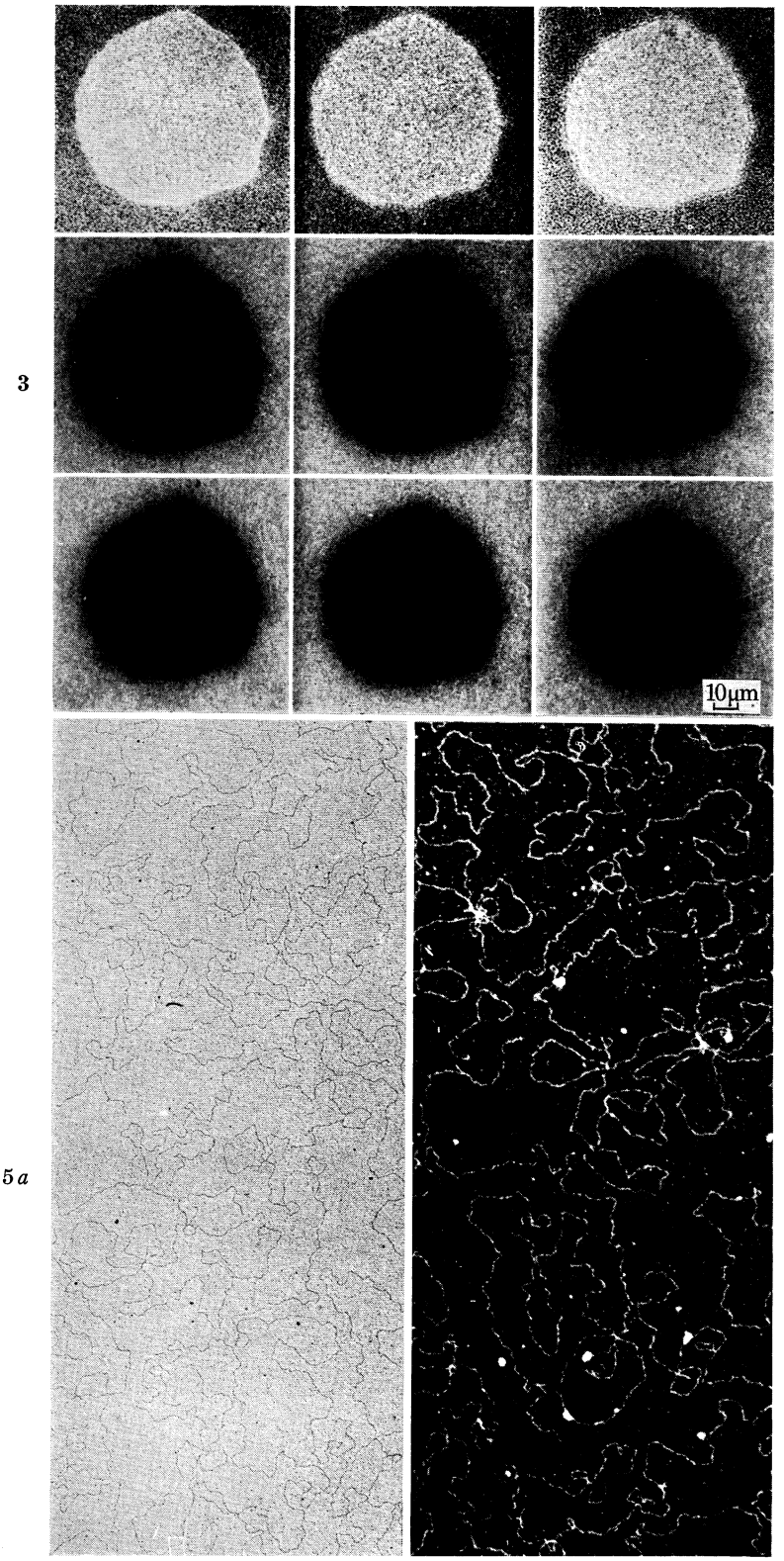

FIGURE 3. A hole (60 nm diameter) in bright field (upper row = three-exposure focus series) and in dark field (lower rows = six-exposure series) photographed at high magnification (100 000×) with the aid of the mechanical beam tilt in the Siemens Elmiskop IA. The centre image of the bright field (upper row, 2nd micrograph) is in focus, its neighbours of the row are in minimum defocused conditions ($\Delta f = \pm 20$ nm). In the six exposures of the dark field (lower rows), the focus cannot be reached properly due to the thick carbon support film. Its brightness and the non-mottled granulated appearance indicates a heavy layer, the edges of which cannot adequately be focused.

FIGURE 5. Electron micrographs of an unstained λ phage DNA-cytochrome *c* film, photographed at about × 6000, total magnification × 26 000 (80 kV, condenser aperture 200 μm). (*a*) Bright-field photography with objective aperture 50 μm in Siemens Elmiskop IA (W. Hellmann). The background in which the DNA filaments can be observed on the screen is granulated. The micrograph of the highest contrast was chosen. (*b*) Dark-field photography of the same DNA-protein monolayer using the magnetic tilting device of the Siemens Elmiskop 101. I am much indebted to Dr E. de Harven (Sloan Kettering Institute for Cancer Research, New York) for this and various other electron micrographs. The exposure time (4 s) requires high stability of the image. The DNA filaments appear clearly and have high contrast at the crossing sites.

(*Facing p.* 146)

PHILOSOPHICAL TRANSACTIONS OF THE ROYAL SOCIETY B BIOLOGICAL SCIENCES

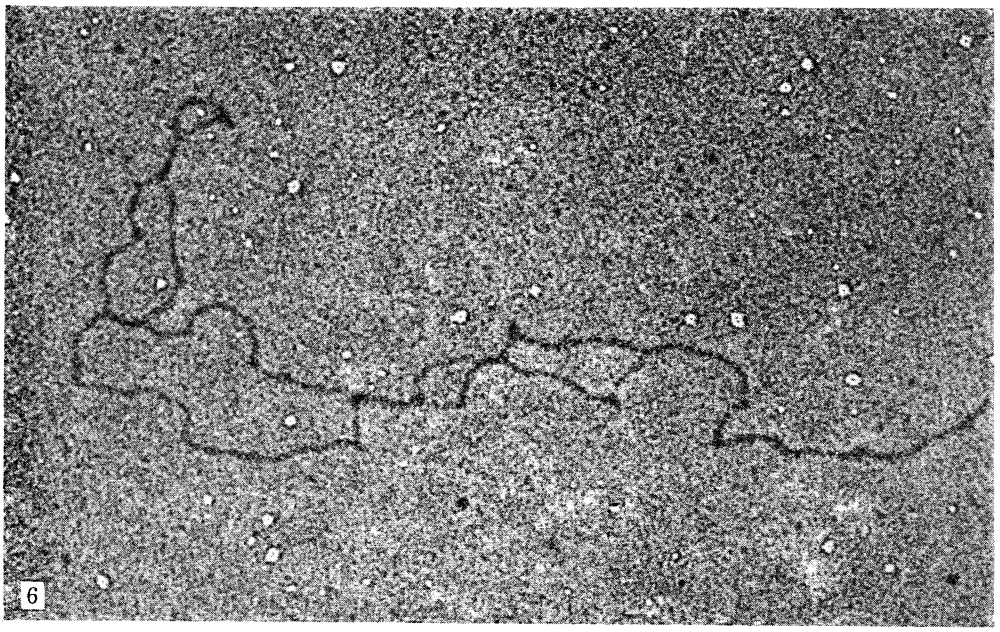

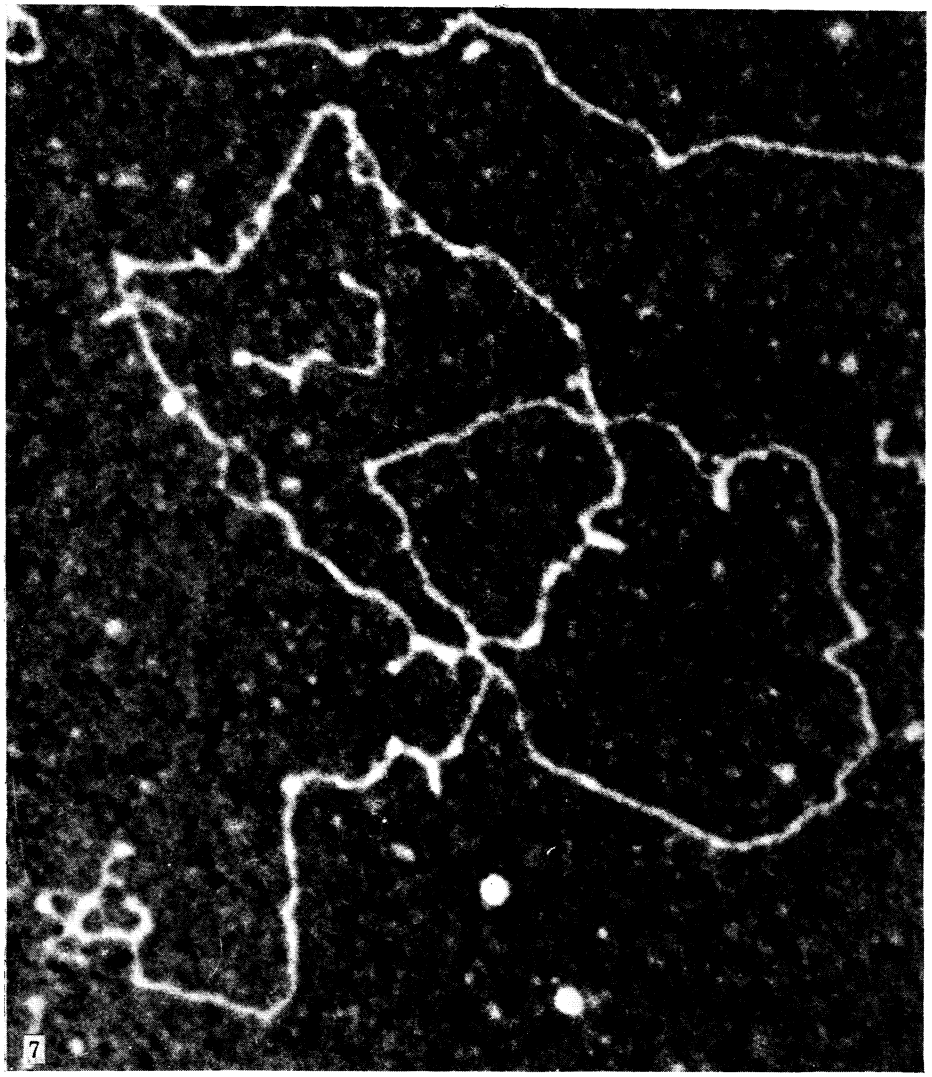

FIGURE 6. Electron micrograph of unstained DNA of adeno-12 virus partly melted by heat-formaldehyde. (Magn. × 92 000.) The protein monolayer of partly melted DNA (Doerfler & Kleinschmidt 1970) is transferred and rinsed with ethanol and dried. After removal of collodion, micrographs are taken at × 12 000 magnification (or lower). The small holes visible in the background of many fields of view show fringes due to the over-focused imaging. Under these conditions, the DNA filaments are in maximal contrast.

FIGURE 7. Dark field image of unstained, partly melted DNA of adeno-12-virus. (Magn. × 90 000.) The DNA filament appears multilooped and collapsed at many sites (formaldehyde-heat denaturation > 50%). The carbon background is mottled and contains many small holes which appear after ethanol treatment of the preparation (see figure 4).

PHILOSOPHICAL TRANSACTIONS OF THE ROYAL SOCIETY B BIOLOGICAL SCIENCES

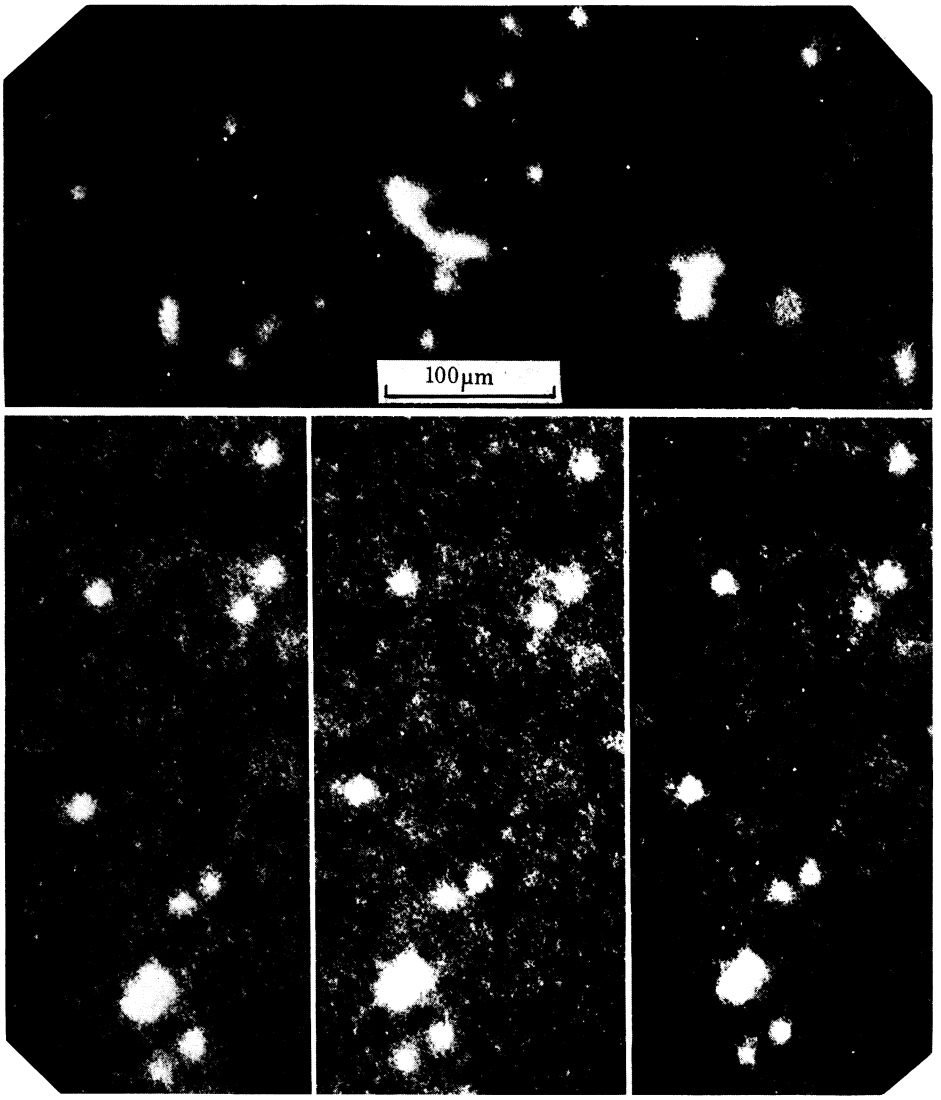

FIGURE 8. Dark-field electron micrographs of horse spleen ferritin. Top: ferritin molecules mounted on a thick carbon support film. Bottom: focus-series of ferritin molecules mounted on thin carbon support film (see text).

PHILOSOPHICAL TRANSACTIONS OF THE ROYAL SOCIETY B BIOLOGICAL SCIENCES

Results

(*a*) DNA-*protein monolayers in bright and dark field*

For study of the gross configuration and detailed fine structure of filamentous macromolecules, the protein monolayer procedures have proved to be very useful (Kleinschmidt 1968). This method has been used for studies of unstained DNA-protein monolayers in bright field (Kleinschmidt & Vasquez 1969) and dark field electron microscopy.

An unstained preparation of λ phage DNA (wild type) is shown in figure 5, plate 27. The bright field survey taken at 80 kV and chosen from a focus series (figure 5*a*) clearly distinguishes in random path and end positions each filament of about 16 μm contour filament length. The carbon support film appears granulated. The background is devoid of the heavily contrasting particles found in high-contrast staining (Gordon & Kleinschmidt 1968). Only a few tangled filaments in the field of view should be excluded from length measurements. At crossing positions, filaments show only slightly increased contrast. A striking feature of all these preparations, however, is the width of the DNA filaments which exceeds considerably the diameter of naked DNA (2 nm). This increase in thickness, first assumed to be caused by metal shadow or high-contrast staining (Gordon & Kleinschmidt 1968), must therefore be due to the complexing of DNA with the protein (e.g. cytochrome *c*). Ethanol treatment, as a final preparation step in transfer (see figure 4), may enhance the apparent width of DNA filaments. This DNA–protein complex of unknown structure will conceal details of the helical or coiled configuration below the range of 10 nm linear dimension.

In dark-field observations (figure 5*b*) of the unstained λ DNA–protein monolayer, the bright contrast of the filaments is striking. Contours and end positions of untangled filaments are easily measurable. The background at the low magnification appears mottled. When the DNA filaments are observed on the electron microscope screen after the eye has adapted to the dark image, it was found that focusing the object on the final screen is far easier than in bright-field observations. The loop crossovers, however, are of much higher contrast in dark field than in bright field which indicates strong scattering by the DNA of double thickness. Furthermore, the background exhibits contaminating particles as heavily scattered small objects of variable size. Internal details of these particles, often seen in bright field, are now missing.

In partly denatured DNA of various origins, it has been shown that the diameter of DNA in double-stranded and single-stranded looped regions does not differ very much in unstained preparations (Kleinschmidt & Vasquez 1969). We have observed a contrast increase at random locations of partly denatured DNA of adeno-2-DNA which was assumed to indicate local collapsed regions in single- or double-stranded filaments (Doerfler & Kleinschmidt 1970). In DNA preparations of adeno-12-DNA, we found a similar contrast enhancement due to the strand separation and local collapse as shown in figure 6, plate 28. The unstained DNA–protein monolayer was mounted on an extremely thin carbon support film which, after ethanol treatment (see figure 4), became holey to variable degrees. Each of the minute holes allows observation of its fringes which indicate that an over-focused position of the support film and the DNA–protein complex is that in which the contrast of filaments is highest (figure 6).

When these observations on extremely thin support films were extended to dark field using a dark-field objective aperture, the extensively denatured DNA (~50% denaturation sites) in the protein monolayer showed multiple collapsed regions, loops of variable size, and many small holes (figure 7, plate 28). Treatment with organic solvents (ethanol, acetone, acetone–

PHILOSOPHICAL TRANSACTIONS OF THE ROYAL SOCIETY B BIOLOGICAL SCIENCES

water) can generate many holes the size and number of which in the carbon support can be influenced somewhat. The cautious removal of collodion by heat (180 °C, 10 min) preserves the support film and preparation. Dissolving the collodion layer by organic solvents, however, leads to instantaneous breakage of the carbon support film. The collapsed regions of DNA indicate that the total length of DNA can shrink to about 30 %, which also was shown in denaturation sites of adeno-2-viral DNA and λ phage DNA (Doerfler & Kleinschmidt 1970).

(*b*) *Nucleoprotein and protein complexes*

Unstained *E. coli* Q 13 and MRE 600 ribosomal subunits were studied in bright field microscopy by droplet methods (Kleinschmidt & Vasquez 1969). The prolate forms of the 30 S subunits often vary from short dense, rod-like particles to triangular-shaped forms of 11 nm maximum diameter. The variable contours of these particles (Vasquez, Miller & Kleinschmidt, in preparation) suggest a high plasticity in the configuration of the non-periodic RNA–protein complex when prepared for electron microscopy. This agrees with the data of the ribosomal structure found in various morphological (see, for example, Lubin 1968) and functional states (see Spirin, Kiselev, Shakulov & Bogdanov 1963; Spirin 1969; Nomura *et al.* 1969; Schlessinger 1969). A ribosomal particle may have undergone major damage in its gross configuration when dried and adsorbed on to the carbon support. Or the different sites of view in which the particle is adsorbed, project contours in the final image which vary according to the internal complex structure of a non-periodic particle. Variation in internal contrast of a collection of particles indicates that probably plasticity, the projection view, and other factors of deformation may influence details in the size and shape of an areal image of 30 s ribosomes.

Similar obstacles exist in observing the 50 s ribosomal subunits. It has been claimed that the 50 s particles exhibit an icosahedral form (Nanninga 1968) observed only in metal-shadowed preparations. Such regular forms could not be seen in unstained 50 s preparations. The polygonal particles obviously are rounded-off and expose in many instances peripheral protuberances and spikes; the areas (about 11 to 15 nm diameter) vary widely (Vasquez *et al.* in preparation) in contours and total contrast.

Preliminary observations in dark field, however, fail to show the structural details of ribosomal subunits seen in bright-field observations, and variable internal contrast is obtained. In dark field, the 50 s particles show bright contours comparable to those of the bright field image. However, detailed internal structure in the peripheral or centre area of the particles could not be observed. For these large particles (mass more than 10^6 daltons), dark-field imaging obviously produces enough contour contrast but not enough contrast variation in the projected views of such aperiodic particles of 30 s and 50 s size. Smaller particles such as transfer RNA or ribonuclease molecules, as Ottensmeyer (1969) has shown, seem at present to be more suitable for dark-field electron microscopy. In their minimum diameters, the linear dimension should not exceed about 10 nm.

Horse spleen ferritin molecules were studied in a similar way by bright- and dark-field electron microscopy. These molecules have an iron content (up to 20 % of the molecular mass of iron-free apoferritin) forming a mineral microcrystalline core (Fischbach, Harrison & Hoy 1969). The apoferritin consists of about 24 protein subunits (Crichton & Bryce 1970) of a total molecular mass between 430 000 and 470 000 daltons. Electron microscopic and chemical studies (Haggis 1966; Williams & Harrison 1968; Richter & Walker 1967) have shown that the

PHILOSOPHICAL TRANSACTIONS OF THE ROYAL SOCIETY B BIOLOGICAL SCIENCES

iron core is easily visualized in bright field and that the monomeric ferritin molecules associated to form oligomers. An unpurified diluted preparation of horse spleen ferritin is shown in figure 8, plate 29. The upper photograph was taken from a preparation on a thick carbon support film while the lower row shows series electron micrographs of dispersed ferritin molecules mounted on an extremely thin carbon support film.

In the upper electron micrograph of figure 8, the influence of a thick support film (estimated to be more than 5 nm) is illustrated by a veiled appearance of the peripheral range of each isolated molecule. The individual molecules vary in size and shape on a faintly mottled background. The mean diameter of 8 nm indicates that the iron core contributes most to the electron scattering, and the peripheral area of the protein is not revealed.

In conclusion, the unstained macromolecules prepared on very thin carbon supports necessitate conditions for electron microscopy which include a perfect dark-field device and high stability of the final image. Bright- and dark-field images of the same object provide a means of evaluating those details of structure which may be concealed by the apposition of positive stains or metal shadows.

My thanks are due to Dr F. Thon for providing us with tripartite dark-field objective apertures of proper thickness, to Dr E. de Harven for enthusiastically studying various dark fields with our preparations, and to the John A. Hartford Foundation, Inc., New York, for a research grant.

References (Kleinschmidt)

Bradley, D. E. 1965 In *Techniques for electron microscopy* (ed. D. H. Day), 2nd edn, p. 71. Philadelphia: F. A. Davis and Co.
Crichton, R. R. & Bryce, C. F. A. 1970 *F.E.B.S. Lett.* **6**, 121.
Doerfler, W. & Kleinschmidt, A. K. 1970 *J. molec. Biol.* **50**, 579.
Dupouy, G., Perrier, F. & Verdier, P. 1966*a* *C. r. hebd Séanc. Acad. Sci., Paris* **262**, 1063.
Dupouy, G., Perrier, F. & Verdier, P. 1966*b* *J. Microscopie* **5**, 655.
Fischbach, T. A., Harrison, P. M. & Hoy, T. G. 1969 *J. molec. Biol.* **39**, 235.
Gordon, C. N. & Kleinschmidt, A. K. 1968 *Biochim. biophys. Acta* **155**, 305.
Haggis, G. H. 1966 *Proc. 6th Int. Cong. Electron Microscopy, Kyoto* 1966, **2**, 127.
Hall, C. E. 1966 *Introduction to electron microscopy*, 2nd edn, p. 257. New York: McGraw-Hill.
Heidenreich, R. D. 1964*a* *Fundamentals of transmission electron microscopy*, pp. 29 ff. New York: Interscience Publishers.
Heidenreich, R. D. 1964*b* *Fundamentals of transmission electron microscopy*, pp. 52 ff. New York: Interscience Publishers.
Kleinschmidt, A. K. 1968 In *Methods in enzymology*, vol. 12 B (ed. L. Grossman and K. Moldave), p. 361. New York: Academic Press.
Kleinschmidt, A. K. & Vasquez, C. 1969 *27th Annual Electron Microscopy Society of America Meeting*, p. 265.
Lang, D. 1970 *Phil. Trans. Roy. Soc. Lond.* B (this volume).
Lubin, M. 1968 *Proc. natn. Acad. Sci., U.S.A.* **61**, 1454.
Nanninga, N. 1968 *Proc. natn. Acad. Sci., U.S.A.* **61**, 614.
Nomura, M., Mizushima, S., Ozaki, M., Traub, P. & Lowry, C. V. 1969 *Cold Spring Harb. Symp. quant. Biol.* **34**, 49.
Ottensmeyer, F. P. 1969 *Biophys. J.* **9**, 1144.
Reimer, L. 1967 *Elektronenmikroskopische Untersuchungs—und Präparations methoden*, 2. Aufl., p. 329. Berlin: Springer.
Richter, G. W. & Walker, G. F. 1967 *Biochemistry* **6**, 2871.
Schlessinger, D. 1969 *Bact. Rev.* **33**, 445.
Shelton, E. & Kuff, E. F. 1966 *J. molec. Biol.* **22**, 23.
Spirin, A. 1969 *Cold Spring Harb. Symp. quant. Biol.* **34**, 197.
Spirin, A., Kiselev, N. A., Shakulov, R. S. & Bogdanov, A. A. 1963 *Biokhimiya* **28**, 920.
Stoeckenius, W. 1970 *Biophys. J.* **10**, 131*a*.
Thon, F. 1968 *Regional European Conference on Electron Microscopy*, p. 127. Rome.
Williams, M. A. & Harrison, P. M. 1968 *Biochem. J.* **110**, 265.

PHILOSOPHICAL TRANSACTIONS OF THE ROYAL SOCIETY B BIOLOGICAL SCIENCES

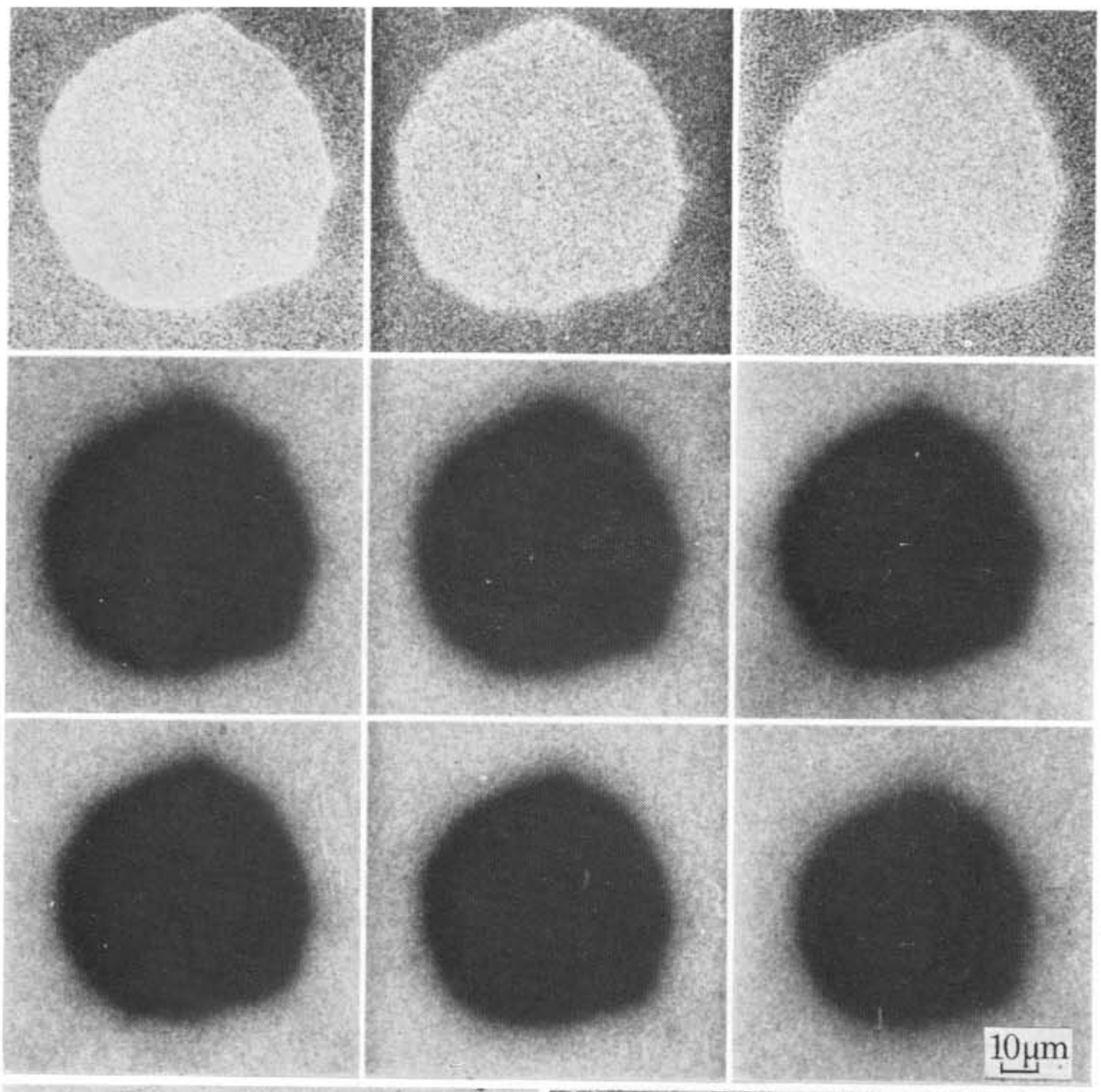

3

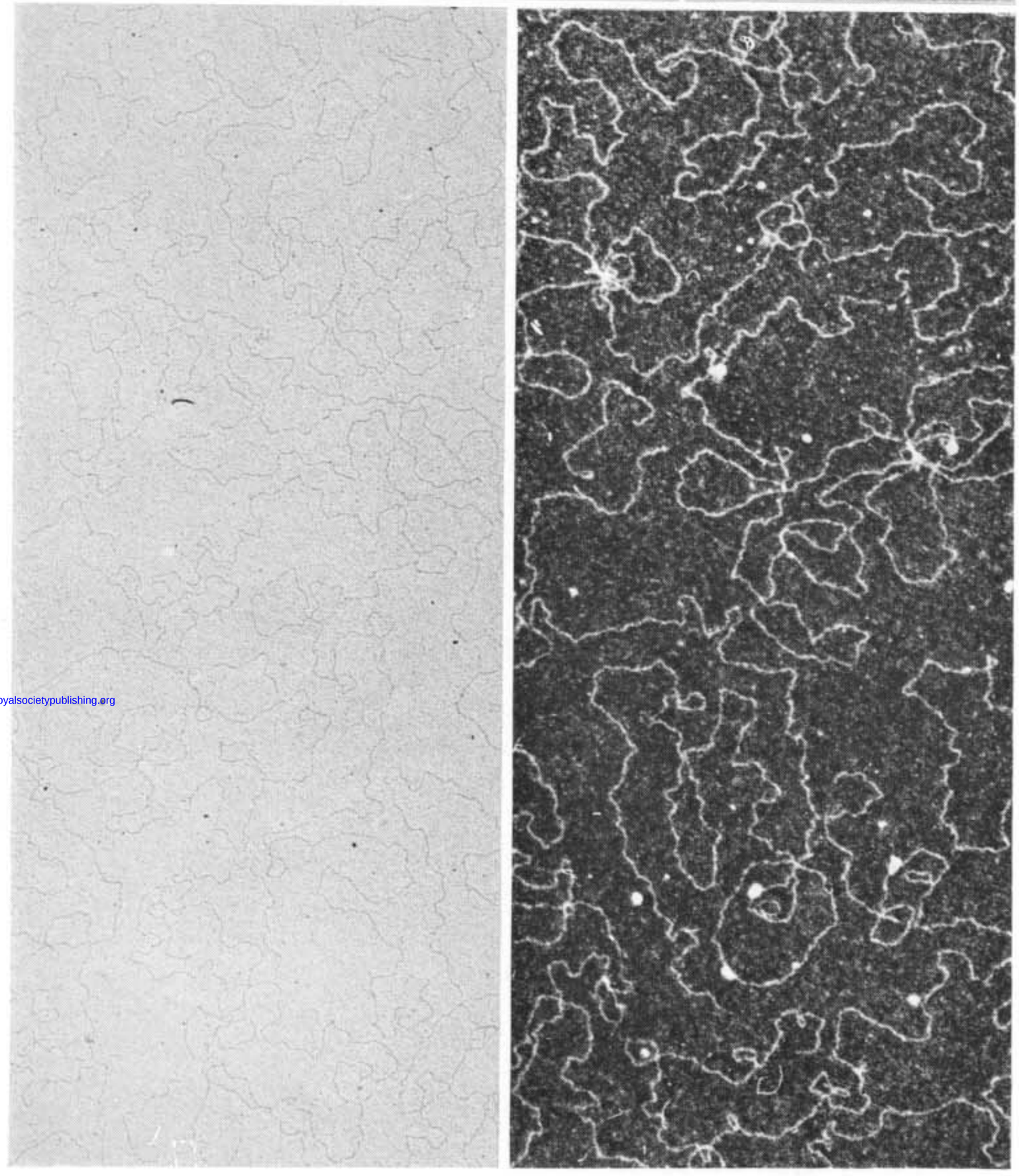

5*a*

5*b*

FIGURE 3. A hole (60 nm diameter) in bright field (upper row = three-exposure focus series) and in dark field (lower rows = six-exposure series) photographed at high magnification (100 000×) with the aid of the mechanical beam tilt in the Siemens Elmiskop IA. The centre image of the bright field (upper row, 2nd micrograph) is in focus, its neighbours of the row are in minimum defocused conditions ($\Delta f = \pm 20$ nm). In the six exposures of the dark field (lower rows), the focus cannot be reached properly due to the thick carbon support film. Its brightness and the non-mottled granulated appearance indicates a heavy layer, the edges of which cannot adequately be focused.

FIGURE 5. Electron micrographs of an unstained λ phage DNA-cytochrome *c* film, photographed at about ×6000, total magnification ×26 000 (80 kV, condenser aperture 200 μm). (*a*) Bright-field photography with objective aperture 50 μm in Siemens Elmiskop IA (W. Hellmann). The background in which the DNA filaments can be observed on the screen is granulated. The micrograph of the highest contrast was chosen. (*b*) Dark-field photography of the same DNA-protein monolayer using the magnetic tilting device of the Siemens Elmiskop 101. I am much indebted to Dr E. de Harven (Sloan Kettering Institute for Cancer Research, New York) for this and various other electron micrographs. The exposure time (4 s) requires high stability of the image. The DNA filaments appear clearly and have high contrast at the crossing sites.

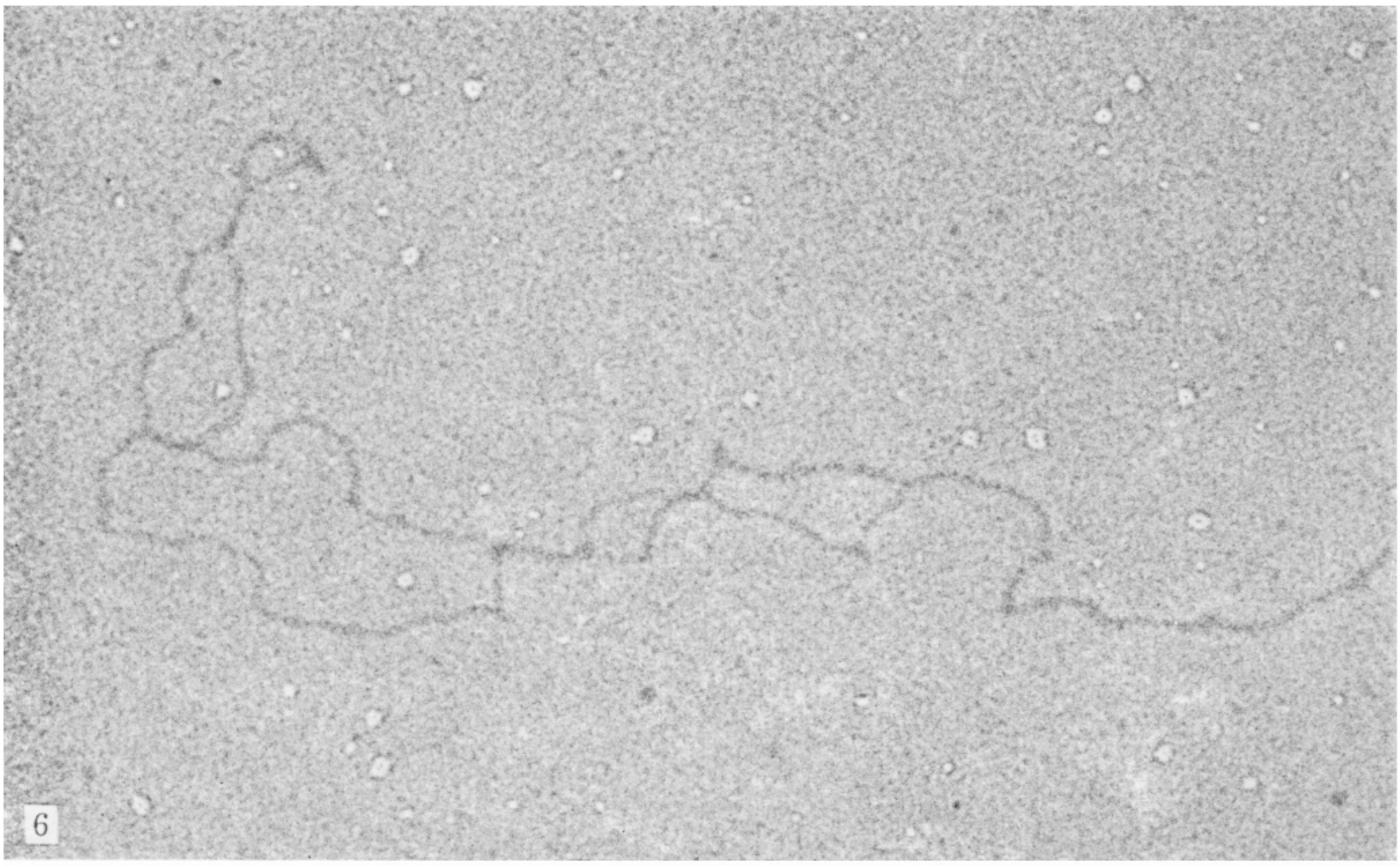

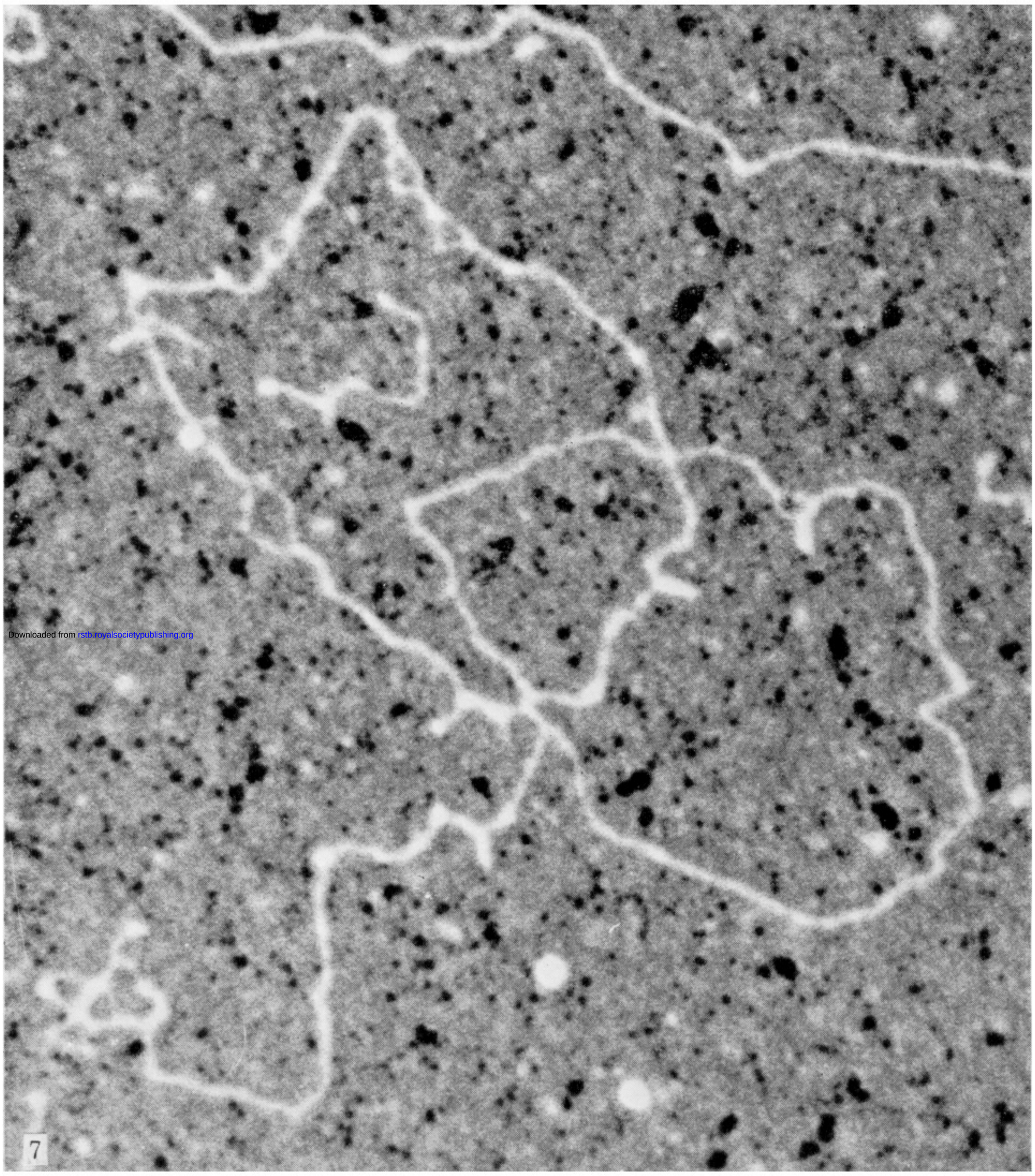

PHILOSOPHICAL TRANSACTIONS OF THE ROYAL SOCIETY B BIOLOGICAL SCIENCES

FIGURE 6. Electron micrograph of unstained DNA of adeno-12 virus partly melted by heat-formaldehyde. (Magn. $\times 92\,000$.) The protein monolayer of partly melted DNA (Doerfler & Kleinschmidt 1970) is transferred and rinsed with ethanol and dried. After removal of collodion, micrographs are taken at $\times 12\,000$ magnification (or lower). The small holes visible in the background of many fields of view show fringes due to the over-focused imaging. Under these conditions, the DNA filaments are in maximal contrast.

FIGURE 7. Dark field image of unstained, partly melted DNA of adeno-12-virus. (Magn. $\times 90\,000$.) The DNA filament appears multilooped and collapsed at many sites (formaldehyde-heat denaturation $> 50\%$). The carbon background is mottled and contains many small holes which appear after ethanol treatment of the preparation (see figure 4).

PHILOSOPHICAL TRANSACTIONS OF THE ROYAL SOCIETY B BIOLOGICAL SCIENCES

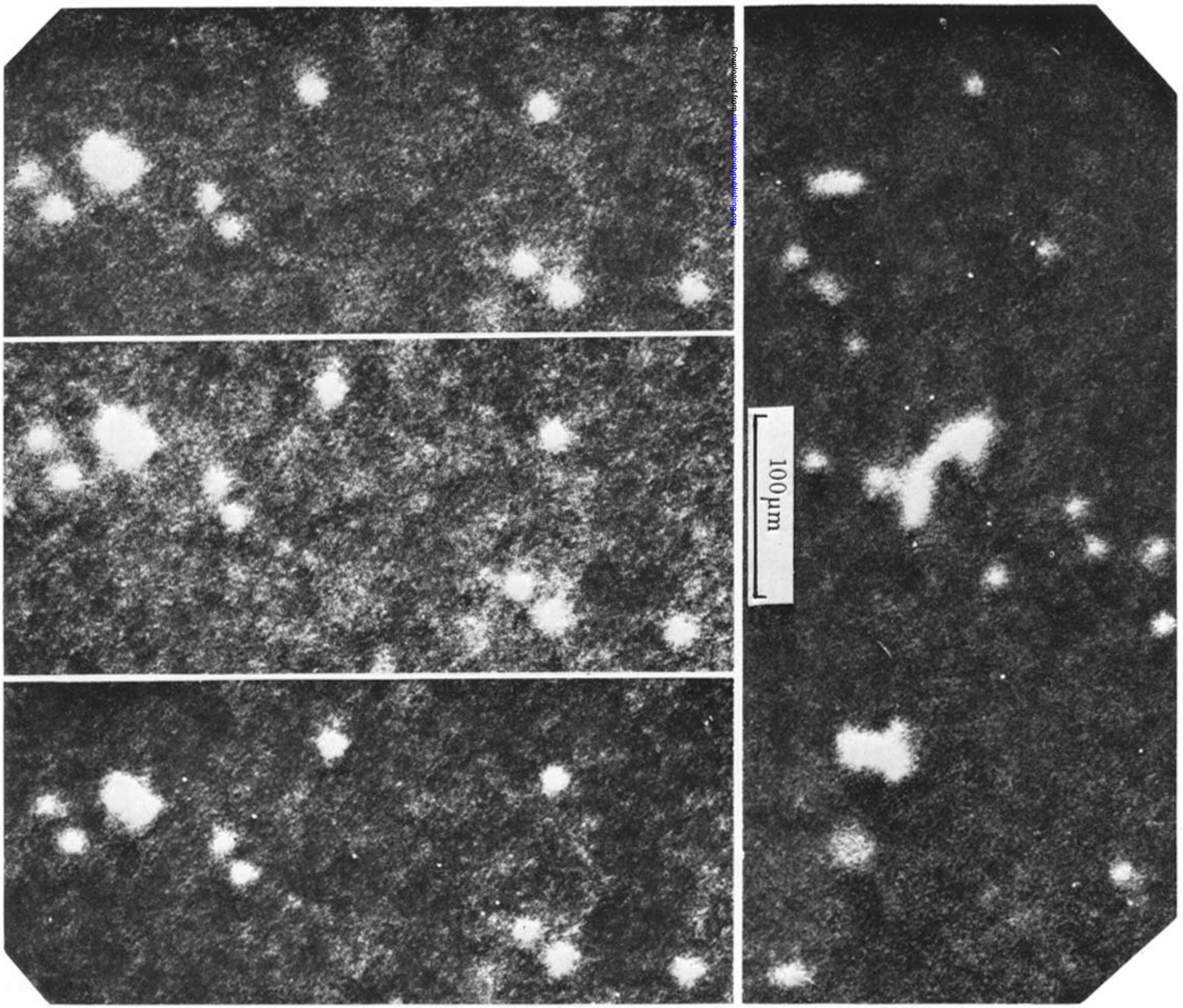

FIGURE 8. Dark-field electron micrographs of horse spleen ferritin. Top: ferritin molecules mounted on a thick carbon support film. Bottom: focus-series of ferritin molecules mounted on thin carbon support film (see text).